Magnetic tunnel junctions

Fueled by the ever-increasing demand for larger hard disk drive storage capacities, extensive research over the past decade has resulted in the development of AlO_x- and TiO_x-based magnetic tunnel junctions that exhibit a large magnetoresistive effect at room temperature. As their commercialization in various applications begins, a new type of magnetic tunnel junction with a crystalline MgO tunnel barrier has emerged that shows a much larger room-temperature magnetoresistive effect. We present a brief overview of the development of magnetic tunnel junctions, introducing the underlying physics. We also discuss two important commercial applications: read sensors in hard disk drives and memory elements in magnetoresistive random access memory. An emphasis is placed on the material aspects of magnetic tunnel junctions.

Jian-Gang (Jimmy) Zhu[1,*] and Chando Park[2]

[1]Data Storage Systems Center, Department of Electrical and Computer Engineering, Carnegie Mellon University, Pittsburgh, PA 15213-3890, USA

[2]Western Digital Corporation, 44100 Osgood Road, Fremont, CA 94539, USA

**E-mail: jzhu@ece.cmu.edu*

Our first knowledge of how to alter the flow of electrons in a metal by directly varying the direction of the local magnetic moment came with the discovery of the anisotropic magnetoresistive (AMR) phenomenon in 1857[1]. More than a century later, the AMR effect found its greatest use in hard disk drive (HDD) read heads for data retrieving, an application that, at the time, was critical for HDDs to meet rapidly growing demands for storage capacity[2]. As the area storage density in HDDs climbed at a compounded growth rate of >60% per year, the demand for a larger magnetoresistive effect ignited extensive research efforts worldwide. This has led to the discovery of the giant magnetoresistive (GMR) effect in 1988[3] and the development of aluminum oxide magnetic tunnel junctions (MTJs) in 1991[4-12] and magnesium oxide MTJs at beginning of the new century[13-23]. Despite these achievements, the research effort continues today.

In this review, we introduce the basic science involved in MTJs and discuss two of their important technological applications: HDDs and magnetoresistive random access memory (MRAM). Material issues important to the two applications are emphasized.

ISSN:1369 7021 © Elsevier Ltd 2006 Open access under CC BY-NC-ND license.

IP Bridge Exhibit 2021
Western Digital v. IP Bridge
IPR2025-00701

Tunnel junctions and magnetic tunnel junctions

When two conducting electrodes are separated by a thin dielectric layer with a thickness ranging from a few angstroms to a few nanometers, electrons can tunnel through the dielectric layer (often referred to as the tunnel barrier) resulting in electrical conduction. As illustrated in Fig. 1, the electron tunneling phenomenon arises from the wave nature of the electrons while the resulting junction electrical conductance is determined by the evanescent state of the electron wave function within the tunnel barrier.

The evanescent transmission of electrons through the tunnel barrier leads to the exponential dependence of the tunneling current with the barrier thickness, as given by the Simmon's expression[24]. Fig. 2 is a graphic illustration of the various parameters used in the equation:

$$I(V) = f(t_b)\left(\left(\bar{\phi} - \frac{V}{2}\right)\cdot e^{-\left(1.025\sqrt{\bar{\phi}-\frac{V}{2}}\right)\cdot t_b} - \left(\bar{\phi} + \frac{V}{2}\right)\cdot e^{-\left(1.025\sqrt{\bar{\phi}+\frac{V}{2}}\right)\cdot t_b}\right) \quad (1)$$

where I is the tunneling current, $\bar{\phi}$ and V are the average tunnel barrier height and bias voltage across the junction in volts, respectively, and t_b is the barrier thickness in angstroms. By measuring the I-V curve of a tunnel barrier and fitting with the Simmon's relation, $\bar{\phi}$ and t_b can be obtained simultaneously.

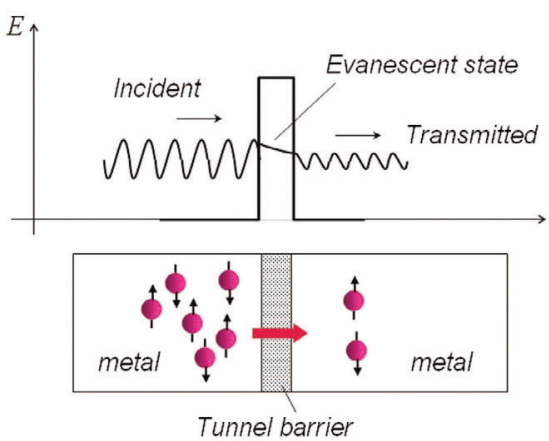

Fig. 1 Electron tunneling through a thin tunnel barrier layer. (Top) The wave nature picture of the tunneling of the electrons. A traveling wave approaching from the left of the barrier. When the barrier height is greater than the energy of the electron, the electron wave inside the barrier layer becomes evanescent as its amplitude decreases exponentially through the barrier. If the barrier layer is thin enough so that the amplitude of the evanescent wave does not completely diminish at the other side of the barrier, a traveling wave reemerges again with the residual amplitude and continues to propagate. (Bottom) The corresponding particle view of the tunneling effect. The amplitude ratio between the transmitted and incident waves determines the probability of an electron tunneling through the barrier.

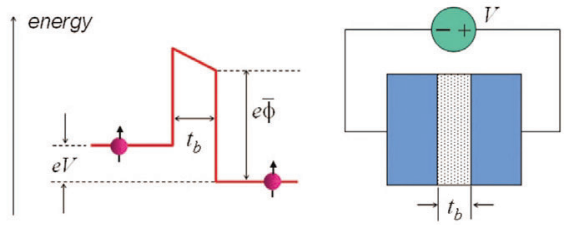

Fig. 2 Illustration of the bias of a tunnel junction and Simmon's I-V relation.

In an MTJ, the two electrodes are ferromagnetic materials. In a ferromagnetic material, an electric current consists of two partial currents, each with either spin-up or spin-down electrons. In a tunneling process in which electron spin is conserved, the tunneling conductance depends on whether the magnetizations M_1 and M_2 of the two electrodes are parallel or antiparallel (Fig. 3). When the relative magnetization orientations are at an angle θ, the conductance becomes proportional to $\cos\theta$ as:

$$G(\theta) = \frac{1}{2}(G_P + G_{AP}) + \frac{1}{2}(G_P - G_{AP})\cdot \cos\theta \quad (2)$$

where G_{AP} and G_P are the conductance for θ = 180° (when the two moments are antiparallel, AP) and θ = 0° (when the two moments are parallel, P), respectively. The corresponding tunneling magnetoresistance (TMR) ratio is defined as:

$$TMR\ Ratio = \frac{G_P - G_{AP}}{G_{AP}} = \frac{R_{AP} - R_P}{R_P} \quad (3)$$

where R_{AP} and R_P are the resistances in the antiparallel and parallel state, respectively.

The origin of TMR arises from the difference in the electronic density of states (DOS) at the Fermi level E_F between spin-up $N_\uparrow(E_F)$

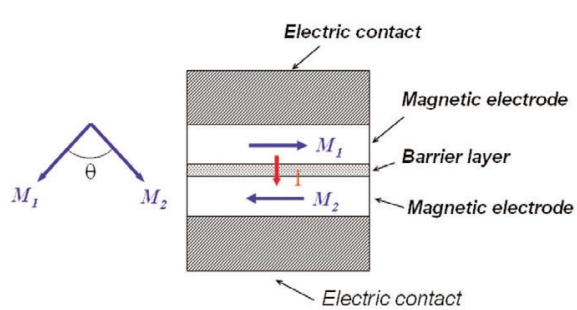

Fig. 3 Schematic showing the magnetizations M_1 and M_2 of the two electrodes in an MTJ. In this case, the magnetizations are in the film plane.

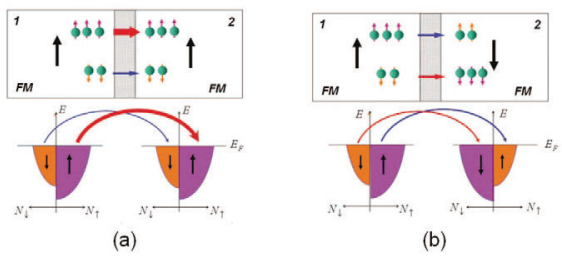

Fig. 4 Schematic of the TMR effect in an MTJ. During tunneling, electron spin orientation is preserved, i.e. an electron can only tunnel to the spin subband of the same spin orientation, and the conductance is proportional to the product of the Fermi level DOS values of the two electrodes of the same spin orientation. A change from the parallel configuration (a) to the antiparallel configuration (b) of the magnetizations of the two electrodes results in an exchange of the spin subband for electrode 2, causing a corresponding change in the conductance.

and spin-down $N_\downarrow(E_F)$ electrons. Since electrons preserve their spin orientation during the tunneling process, electrons can only tunnel into the subband of the same spin orientation, as illustrated in Fig. 4. Thus, the tunneling conductance is proportional to the product of the Fermi level DOS values of the two electrodes with same spin orientation. A change from the parallel magnetization configuration (Fig. 4a) to the antiparallel configuration (Fig. 4b) of the two electrodes will result in an exchange between the two spin subbands of one of the electrodes for the tunneling process. Consequently, a corresponding change in the conductance will be seen, provided that the Fermi-level DOS values are different for the two spin subbands.

Using the definition of TMR ratio given by eq 3, the following relation was first obtained by Julliere[27]:

$$TMR\ Ratio = \frac{2P_1P_2}{1-P_1P_2} \tag{4}$$

where P_1 and P_2, defined below, are the polarization factors for the two electrodes, respectively. The polarization factors are defined as[28,29]:

$$P = \frac{N_\uparrow(E_F) - N_\downarrow(E_F)}{N_\uparrow(E_F) + N_\downarrow(E_F)} \ . \tag{5}$$

Julliere[27] first demonstrated the TMR effect experimentally in 1975, measuring a TMR ratio of 14% in a Fe/Ge/Co junction at 4 K. Two decades later, experimental studies found that MTJs with an amorphous AlO_x tunnel barrier exhibit significant TMR ratios at room temperature[4], with values exceeding 15% obtained at room temperature for Co/AlO_x/Co tunnel junctions[6]. Over the following decade, extensive research on aluminum oxide barriers yielded a steady increase in the TMR ratio by finding electrodes with higher spin polarization factors and improving the quality of barrier through

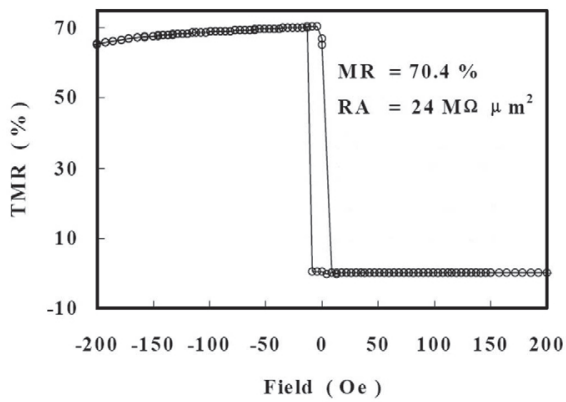

Fig. 5 TMR ratio for an MTJ with the structure Si(100)/Si_3N_4/Ru/CoFeB/Ta/CoFeB/Al_2O_3/CoFeB/Ru/FeCo/CrMnPt at room temperature. The data represents the highest room-temperature TMR ratio ever reported for an amorphous AlO_x MTJ[12]. The applied field change (horizontal axis) results in a change between the parallel state (lower resistance values) and the antiparallel state (higher resistance values). RA denotes the resistance-area product in the parallel state. (Courtesy of D. Wang et al. Reprinted with permission from[12]. © 2004 IEEE.)

the introduction of various material processing procedures. In 2004, a TMR ratio of 70% was achieved using a CoFeB/AlO_x/CoFeB junction made with a standard sputtering technique and a CoFeB target composition of $Co_{60}Fe_{20}B_{20}$ (Fig. 5). Using eq 4, a polarization factor P = 0.61 is obtained for the CoFeB electrode.

In 2001, a series of theoretical calculations predicted extremely high TMR ratios for Fe/MgO/Fe MTJs, where the tunnel barrier is a crystalline MgO layer with (001) texture[13,14]. The study argued that a coherent lattice matching between the (001) plane of body-centered cubic (bcc) Fe and the (001) plane of MgO results in a spin-dependent match between the evanescent states within the tunnel barrier and the electronic states of the Fe electrodes. Consequently, the tunneling could become highly spin-dependent. In 2004, two independent experimental investigations, one using a molecular beam epitaxy (MBE) thin-film growth technique and the other using a conventional sputtering technique with specialized underlayer texturing, showed greater than 180% and 220% TMR ratios at room temperature, respectively[18,19]. Encouraged by these two studies, a surge in research quickly followed, seeking even higher TMR ratios (Fig. 6). It still continues to this day, with the most recently reported room-temperature TMR ratio exceeding 400% in a Co(001)/MgO(001)/Co(001) tunnel junction with an estimated polarization factor P = 0.82.

MTJs with amorphous barrier layers

One of the most extensively studied amorphous tunnel barrier layers is aluminum oxide because of its suitability for forming a thin (~10 Å), smooth, and dense barrier layer, along with its relatively high bonding

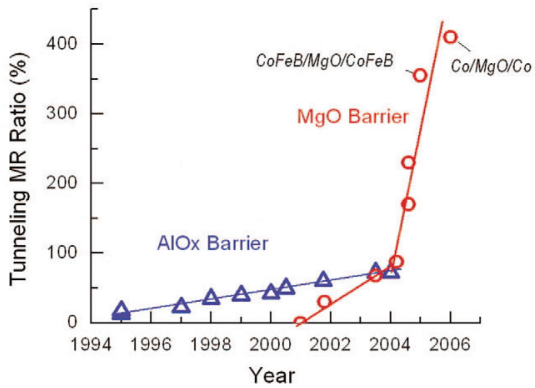

Fig. 6 Reported room-temperature TMR ratios over the past decade for amorphous AlO_x-based MTJs (blue triangles) and crystalline MgO-based MTJs (red circles). (Sources: www.aist.go.jp and references[4-23].)

energy with oxygen (>3 eV). Using various physical vapor deposition techniques, such as sputtering and ion beam deposition (IBD), the tunnel barrier can be formed by depositing a thin Al layer followed by oxidation. Creating a plasma at the sample surface to enhance the oxidation of the Al layer often produces a tunnel junction with higher TMR values than with natural oxidation; however, it also results in a higher resistance-area product (*RA*) value because of the higher barrier height[30,31]. A typical AlO_x-based MTJ has a barrier height ranging from 0.7-1 eV for barriers formed by natural oxidation and 1-3 eV for those formed by plasma oxidation. Furthermore, postannealing is often needed to obtain high TMR ratios[8]. Adequate oxidation of the Al layer to produce a tunnel barrier is critical, either under- or over-oxidation usually leads to significant degradation of the TMR ratio. Fig. 7 shows a transmission electron micrograph (TEM) of a Fe/AlO_x/NiFe tunnel junction, with the amorphous nature of the tunnel barrier evident.

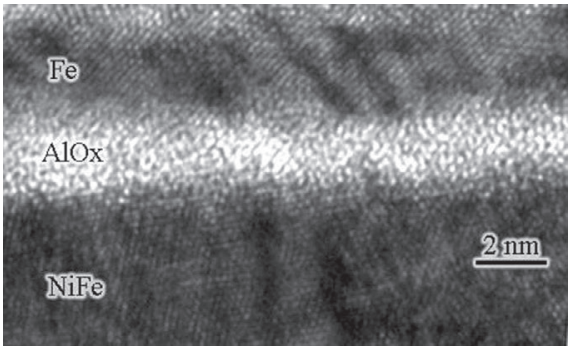

Fig. 7 TEM image of a Fe/AlO_x/NiFe tunnel junction fabricated using a sputtering technique. The AlO_x tunnel barrier is formed by depositing Al followed by a plasma-enhanced oxidation process.

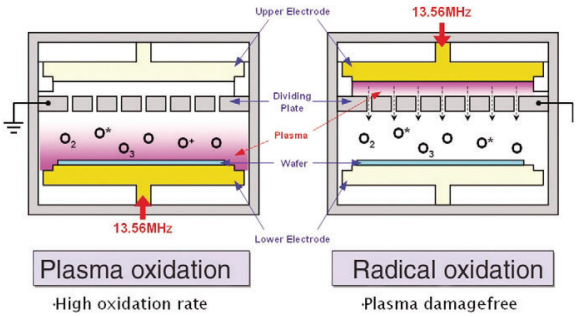

Fig. 8 Plasma-enhanced oxidation process (left) and radical oxidation process (right), where the plasma is kept away from the substrate. (Courtesy of Ki-seok Moon.)

Another amorphous tunnel barrier material that has been studied extensively is TiO_x because of its relatively low barrier height, ~100 meV[32,33]. Such a low barrier height value enables low *RA* product values, ~1 Ω μm^2, at not-so-thin barrier thicknesses, a property of particular interest for many applications, especially in HDD read heads. To produce an adequate TiO_x tunnel barrier, a particular oxidation process on a deposited Ti layer is required, known as the radical oxidation process (Fig. 8). Compared with natural oxidation, radical oxidation provides more thorough oxidation of the Ti layer, while compared with plasma-enhanced oxidation, it leaves the barrier free of any possible plasma-induced damage.

Both AlO_x- and TiO_x-based MTJs can be fabricated by commonly used sputtering techniques, which enable robust manufacturability. Both are currently used in commercial products as discussed later in this review.

MTJs with crystalline MgO barrier layers

As discussed previously, achieving a high TMR ratio in MgO-based MTJs requires correct crystalline orientation of the ferromagnetic electrodes, which are either bcc Co, bcc Fe, or an alloy of the two, and lattice matching at the interfaces between the electrodes and the tunnel barrier. However, it has proven difficult to grow bcc Co or bcc Fe with (001) texture directly by any practical physical vapor deposition technique without a single crystal substrate (the use of which would vastly limit commercial applications).

The development of CoFeB/MgO/CoFeB tunnel junctions by Anelva[21] provides a practical solution to overcome this difficulty. In this technique, a $(CoFe)_{80}B_{20}$/MgO/$(CoFe)_{80}B_{20}$ multilayer is deposited using conventional sputtering. At 20% B content, the as-deposited $(CoFe)_{80}B_{20}$ film layer is amorphous in nature. A thin MgO layer grown on top of an amorphous $(CoFe)_{80}B_{20}$ layer can readily achieve a well-oriented (001) texture. Postannealing of the film stack at temperatures around 360°C induces crystallization of the two $(CoFe)_{80}B_{20}$ layers, which occurs epitaxially from the two MgO interfaces. In this way, the

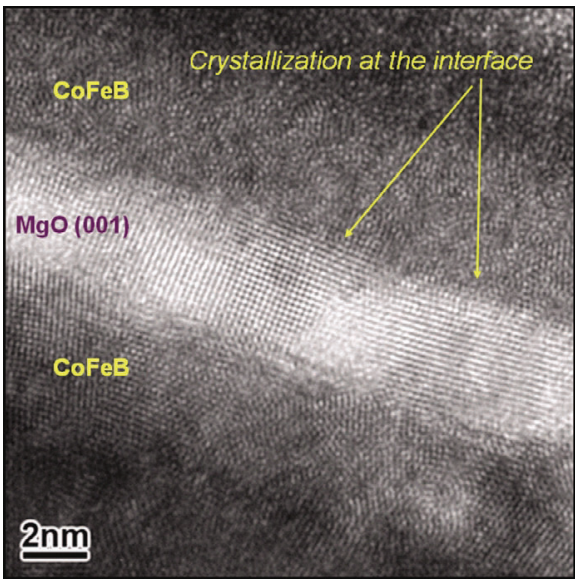

Fig. 9 TEM image of a CoFeB/MgO/CoFeB MTJ deposited using a sputtering technique followed by postannealing at 270°C. The as-deposited CoFeB is purely amorphous while the directly deposited MgO layer clearly shows a well-oriented (001) texture. After the annealing process, the two CoFeB layers form a bcc crystalline structure epitaxially from the interface with the MgO lattice. The measured room-temperature TMR ratio of this particular MTJ is ~110%[34].

crystallized CoFeB at the barrier interfaces can have a bcc structure well matched with the MgO lattice (Fig. 9)[34]. Using this method, TMR ratios well over 350% have been achieved[22].

MTJs with magnetization perpendicular to plane

Materials with high spin-polarization factors usually have correspondingly high saturation magnetizations. Thin films of these magnetic materials naturally have their magnetization oriented in the film plane to avoid magnetic poles at the surfaces. However, many applications demand magnetization to be perpendicular to the film plane, such as perpendicular MRAM designs (discussed later in this review). In order to force perpendicular magnetization, the field generated from the surface magnetic poles, known as the demagnetizing field, needs to be countered. This can be accomplished by using magnetic materials with magnetocrystalline anisotropy, an effective magnetic 'field' resulting from the material's crystalline structure that forces the magnetization to be oriented along certain crystalline axes.

Fig. 10 shows a schematic of a perpendicular MTJ structure. Each magnetic electrode is a bilayer consisting of a thin magnetic layer with

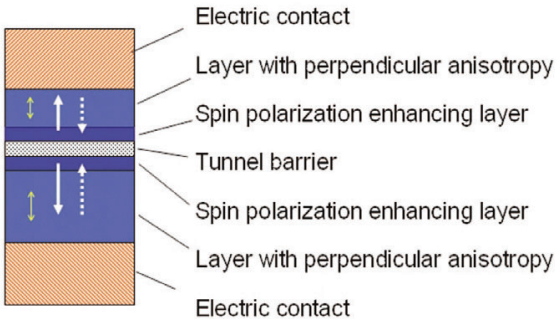

Fig. 10 Schematic of a perpendicular MTJ structure. Each magnetic electrode is a coupled bilayer consisting of a thinner ferromagnetic layer with high spin polarization factor, which has an interface with the tunnel barrier, and a thicker ferromagnetic layer with strong perpendicular magnetocrystalline anisotropy.

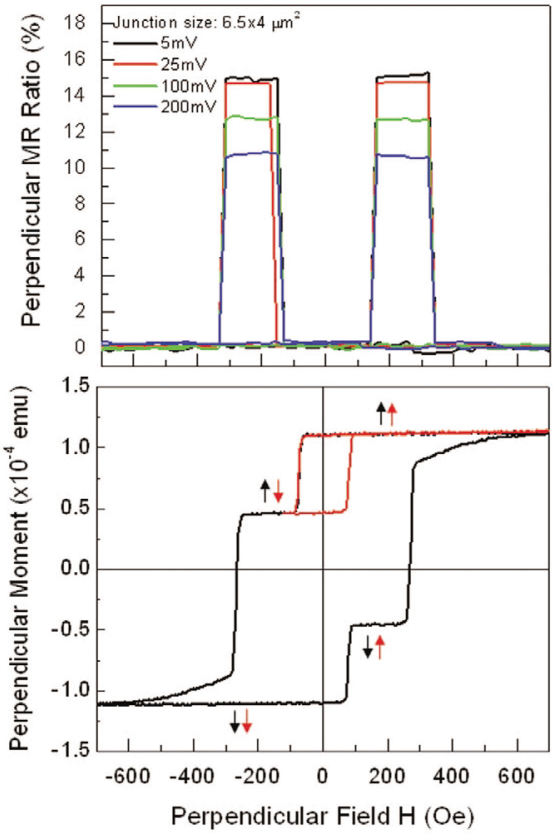

Fig. 11 (Top) Measured room-temperature TMR ratio of a perpendicular MTJ as a function of a perpendicular external magnetic field. The top electrode has the structure, starting from the barrier interface, Co(7 Å)/[Pt(18 Å)/Co(7 Å)]$_2$. The bottom electrode, starting from the Si substrate, has the structure Ta(30 Å)/Pt(50 Å)/[Co(6 Å)/Pt(18 Å)]$_4$/Co(8 Å). The tunnel barrier is a 20 Å thick AlO$_x$ layer formed by a plasma oxidation process. The MTJ has been patterned into a 6.5 x 4 μm^2 area using optical lithography. (Bottom) Corresponding perpendicular magnetic hysteresis curve of the unpatterned structure[36].

a high polarization factor, which interfaces with the tunnel barrier, and a relatively thick magnetic layer with strong perpendicular magnetocrystalline anisotropy. The magnetization of the two layers within the bilayer is strongly coupled through the ferromagnetic exchange energy at their interface. A sufficient volumetric difference between the two layers can force the magnetization of the thinner layer to be completely perpendicular to the film[35].

Fig. 11 shows a series of measured TMR curves for a perpendicular MTJ as a function of an external field applied along the perpendicular direction. The magnetic layers with perpendicular anisotropy are made of a $(Co/Pt)_n$ superlattice, which yields relatively strong perpendicular anisotropy, where the number of repeats *n* is chosen to be different for each of the two electrodes so that they have different anisotropy strengths. Because of the perpendicular anisotropy, reversing the magnetization direction in each electrode requires the external field to exceed a threshold, referred to as the switching field threshold. The difference between the switching field thresholds for the two magnetic electrodes enables well-defined parallel and antiparallel states to be reached.

The different TMR curves in Fig. 11 show measurements at different applied bias voltages. Note that an increase of the bias voltage yields a reduction of the TMR ratio, a common behavior in all MTJs. The rate of TMR degradation with bias voltage magnitude depends on the barrier height, the quality of barrier, and other material properties. Various mechanisms for TMR ratio reduction with bias voltage have been suggested[37]. This behavior means the bias voltage needs to be optimized to maximize the voltage output resulting from the magnetoresistance change.

Application of MTJs in HDD read heads

One of the commercial applications of MTJs is in HDD read heads[38-44]. In September 2004, Seagate Technology shipped the first HDD product with read heads made of TiO_x-based MTJs (Momentus II; a 120 GB, 2.5" drive). Following the move, other disk drive and component companies have begun to commercialize their own MTJ read heads. Today, many disk drive products have read heads with either AlO_x- or TiO_x-based MTJs.

The detailed structure of an MTJ read head in an HDD is illustrated in Fig. 12[2]. One of the magnetic electrodes of the tunnel junction, referred to as the free layer, senses magnetic flux from the magnetic disk medium in a rotation of its magnetization in response to the flux. The other magnetic electrode is known as the reference layer. Its magnetization orientation is 'fixed' in the vertical direction to the disk surface by being next to a multilayered structure consisting of a thin metallic interlayer, a pinned layer, and an antiferromagnetic layer. The magnetic moment orientation of the pinned layer is constrained by an effective surface magnetic field, known as an exchange bias field, which arises from the interface with the antiferromagnetic layer. The purpose of the pinned layer is to compensate the stray field from the reference layer. Hence, the

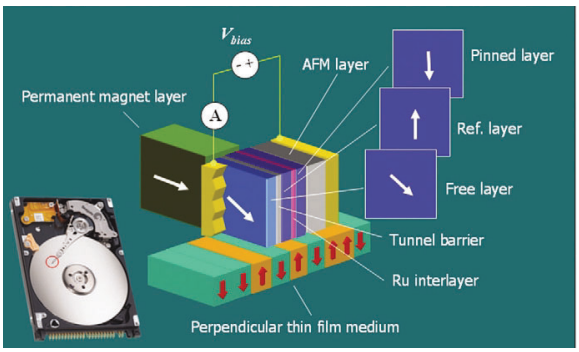

Fig. 12 MTJ read head in an HDD. One magnetic electrode is a free layer, and its magnetization rotates freely in response to the medium signal field. The magnetic moment of the other electrode is 'fixed' through the interlayer magnetic coupling and functions as a reference to the free layer magnetization orientation.

magnetic moment of the pinned layer is always opposite to that of the reference layer. This is done by introducing a strong antiparallel coupling between them by choosing a particular metallic interlayer of adequate thickness. The resulting trilayer – the reference layer, interlayer, and pinned layer – is often referred to as a synthetic antiferromagnet (SAF). A practical SAF in use is CoFe(~25 Å)/Ru(8 Å)/CoFe(~25 Å). The junction stack is sandwiched in between two soft magnetic shields in the downtrack direction (not shown in the illustration) for sufficient spatial resolution[2]. A pair of permanent magnets (only shown on one side here) in the crosstrack direction maintain the single domain state of the free layer in the MTJ. Fig. 13 shows TEM images of MTJ read heads used in present HDD products viewed from the air-bearing surface (ABS).

For MTJs used in HDD read heads, one of the important requirements is a sufficiently low *RA* product value. As the width of the data track continues to decrease so that we can pack more and more data tracks on a disk, the width and height of the MTJ element needs to be reduced accordingly, consequently causing the resistance of the element to increase. Higher head resistance causes higher Johnson noise and shot noise and, more importantly, results in a larger time constant and limited data rate. TiO_x tunnel barriers are often used since a lower *RA* value can be obtained than for AlO_x-based MTJs without having to make the barrier layer so thin that manufacturing becomes difficult.

In the not-so-distance future, HDD read heads are very likely to use MgO-based MTJs. Although MgO has an extremely high TMR ratio compared with those using amorphous barriers, the *RA* product value is an equally important parameter to consider. The two parameters are related in the following way: reducing the *RA* product to below a certain critical value always yields a steep reduction in the TMR ratio, although the critical *RA* product value can be reduced by optimizing processing conditions. This is clearly demonstrated in the two sets of

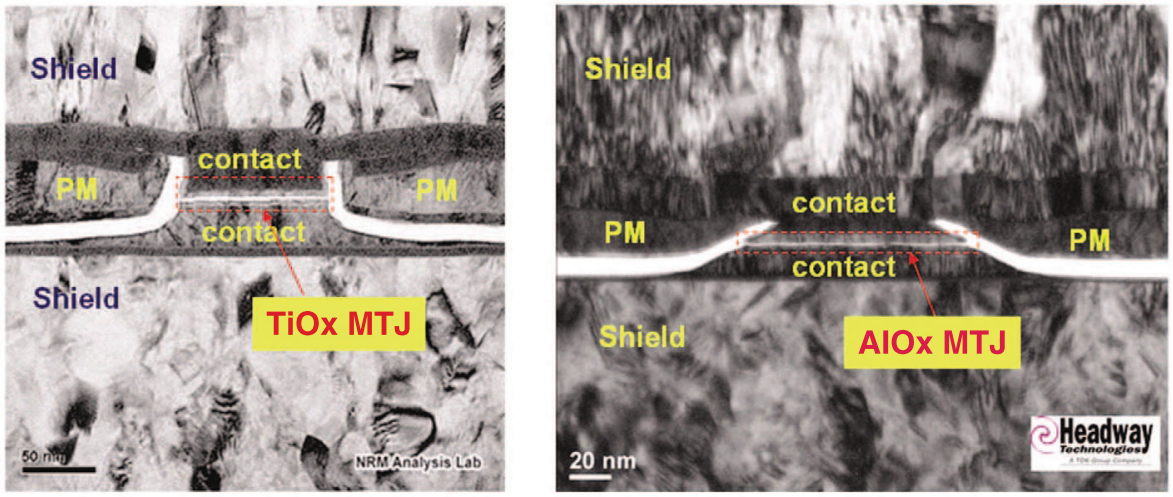

Fig. 13 TEM images of two commercial MTJ read heads. (Left) TMR head with a TiO_x barrier layer produced by Seagate Technology. (Courtesy of Sining Mao.) (Right) TMR head with AlO_x barrier layer produced by Headway Technologies. (Courtesy of Moris Dovek).

experimental data in Fig. 14. Adequate Ar pressure during the MgO layer deposition proves to be critical in achieving low *RA* values while maintaining a relatively high TMR ratio[22]. It has also been reported that depositing a thin Mg layer prior to the deposition of MgO helps the MgO layer to establish quickly the necessary (001) texture at the beginning of the growth so that the optimum TMR ratio can be achieved with a thinner MgO layer[23].

With the data rate of present HDDs already exceeding 1 Gbit/second, the head resistance needs to be maintained at ~200 Ω. Besides reducing the *RA* product, a shunt resistance connected in parallel with a MTJ could be used to maintain the total resistance of the head at a low value. Thus, a higher TMR ratio is required because of the accompanied shunting of signal voltage. Fig. 14 shows the required TMR ratio with the shunt resistance to keep the head resistance at 200 Ω as a function of MTJ *RA* product for various area recording densities.

For a read head, the magnetization of the free layer needs to be sufficiently 'free' in response to the signal flux from the recorded disk medium. This requires a sufficiently low magnetostriction coefficient, a parameter that measures the mechanical stress induced constraint on the direction of magnetization orientation. However, materials with relatively high spin polarization, such as Co, Fe, and CoFeB, have relatively high magnetostriction coefficients. A common approach is to make the free layer a composite free layer with a thin, high-spin polarization layer next to the barrier layer and a relatively thick layer of $Ni_{81}Fe_{19}$ alloy, which has zero magnetostriction coefficient. The two layers usually couple ferromagnetically and act as a single magnetic entity. The composite free layer scheme has been successfully used in the read heads in present commercial HDD products with either AlO_x- or TiO_x-based MTJs. However, it has been a challenge to use the scheme for CoFeB/MgO/CoFeB-based MTJs, as annealing at 360°C is usually required to yield epitaxial crystallization of the CoFeB at the

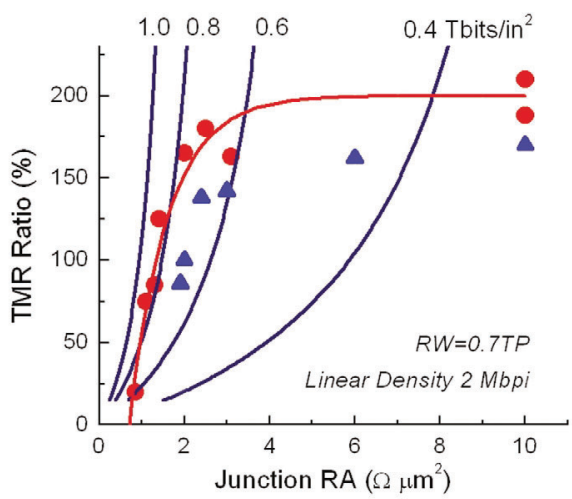

Fig. 14 Required TMR ratio of MTJs as a function of the RA product value for various area storage densities. The calculation assumes an MTJ with an area equal to the square of the read track width (RW), which is 70% of the track pitch, and a shunt resistance connected in parallel to produce an overall head resistance of 200 Ω. A linear density of 2 Mbit/inch (Mbpi) is also assumed. Red circles show data from[22] and blue triangles from[21].

interface with the MgO barrier to give a high TMR ratio. In using a composite free layer together with the tunnel barrier in NiFe/CoFeB/MgO MTJs, epitaxial crystallization from the interface between NiFe and CoFeB occurs during the annealing process at an overwhelmingly faster rate, often leading to destruction of the intended epitaxial crystallization of CoFeB at the MgO barrier interface.

Application of MTJs in MRAM

Another important technological application is the use of MTJs as memory elements in MRAM devices[45-49]. In a computer, the memories that directly provide data bits to the microprocessor are semiconductor devices known as the static random access memory (SRAM) and dynamic random access memory (DRAM). They are fast but need power to maintain the stored bits. When you turn off your PC, the information stored in these memory devices vanishes. The only archival memory in a computer today is HDD. Its access time, however, is six orders of magnitude slower than that of SRAM, as seen in the all too familiar wait when we first turn on our computers.

A new type of memory, based on the magnetoresistive effect and known as MRAM, has been in development over most of the past decade. MRAM is capable of the speed of SRAM, the density of DRAM, and is nonvolatile just like an HDD. MRAM could be the 'dream memory' since it has the potential to replace all the existing memory devices in a computer. This 'universal' memory then becomes an enabling technology for integrating a computer system on a single chip.

Fig. 15 shows a schematic view of two types of memory elements: a conventional, single-storage-layer memory element (left) and a toggle MRAM memory element with an SAF storage layer (right). The memory element is elliptical in shape, which introduces a shape anisotropy with the easy axis along the long axis. Additional uniaxial magnetic anisotropy can be introduced by depositing the film layers in a magnetic field. With the uniaxial magnetic anisotropy, the magnetization orientation of the storage layer becomes binary, forming either a parallel '0' state or an antiparallel '1' state for the magnetization configuration of the magnetic layers adjacent to the tunnel barrier.

For the conventional memory element, switching between the '1' and '0' states of a selected element is achieved using magnetic fields generated by two, temporally coincident current pulses in the *x*- and *y*-write lines that intersect the element. The elements away from the intersection, but under or over either one of the activated current lines, are known as half-selected elements and experience the write magnetic field from one of the current lines. Eliminating erroneous switching for half-selected elements during a write operation has proven to be difficult. Consequently, a commercial product based on this design has not been produced despite extensive research and development efforts.

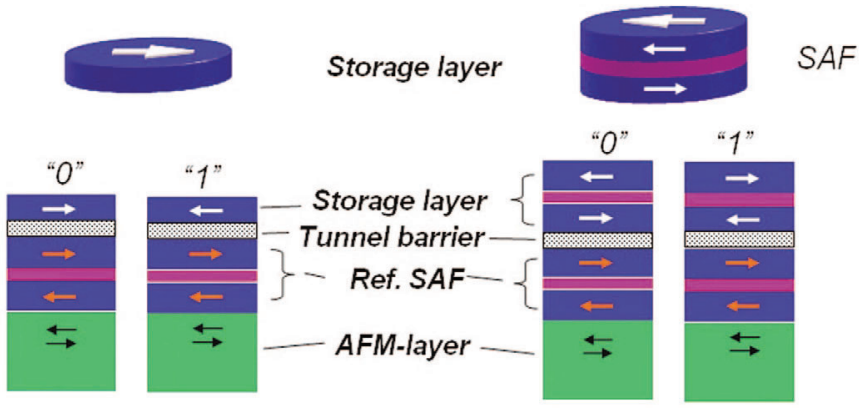

Fig. 15 (Left) Conventional memory element design with a single storage layer. (Right) Toggle memory element with an SAF storage layer. The elliptically shaped elements introduce a uniaxial anisotropy with the easy axis along the elongation, resulting in two well-defined states where the magnetization of the storage layer is either parallel or antiparallel to that of the reference layer. (The storage layer is the magnetic layer next to tunnel barrier in the case of the SAF storage layer.)

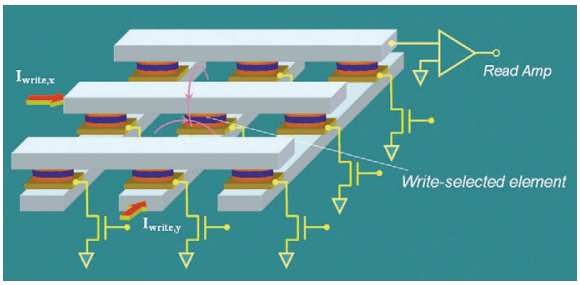

Fig. 16 Schematic of an MRAM memory element array. For the toggle MRAM design, the long axis of the elliptically shaped element is oriented diagonally with respect to the x-y grid of write lines. Each memory element is connected to a designated transistor, which performs the function of read selection.

Freescale's toggle MRAM design is the only commercial success to date with a 4 Mbit chip already in production. The storage layer of the memory element is a magnetic-flux-matched SAF with the easy axis oriented at a 45° angle to the two orthogonally arranged current lines. The current pulses on the two write lines are offset in time such that, in sequence, they produce a full 180° rotation of the magnetic moments in the SAF storage layer of the write-selected element (Fig. 16). A single current field only yields a small magnetization rotation in the SAF storage layer that is fully reversible after the current pulse. In this scheme, erroneous switching of half-selected elements is completely eliminated.

Writing by spin torque

In an MTJ, the tunneling current arriving at the storage layer is spin polarized, i.e. the population of the tunneling electrons with one sign of spin is more than the other (Fig. 17). The net spin moment of the tunneling current is proportional to both the degree of the polarization and the current density, and can generate a torque, referred to as spin torque, on the local magnetization. Depending on the direction of the tunneling current, the effect of the spin torque is to switch the storage layer magnetization to be either parallel or antiparallel to the magnetization of the reference layer[50-55].

Instead of using a magnetic field, spin torque can be used to switch the magnetic moment direction in MRAM memory elements by directly injecting the current through the MTJ. Since the first demonstration of spin-torque-induced magnetic switching in 1999, the topic has become an exciting research frontier with substantial effort devoted to reducing the current density threshold for magnetic switching. In 2005, Sony performed the first on-chip demonstration of a spin-torque-operated nonvolatile memory device, a 4 kbit MRAM device named spin-RAM. In the demonstration, the memory elements (Fig. 18) are CoFeB/MgO/CoFeB MTJs with a TMR ratio >160% and a *RA* product of 20 Ω μm^2. Because the breakdown voltage of an MTJ is usually on the order of a volt[56], a relatively low *RA* product is important so that sufficient current density can be reached without stressing or damaging the tunnel junction.

MRAM elements with in-plane magnetization mainly rely on the shape anisotropy for forming two distinctive memory states with

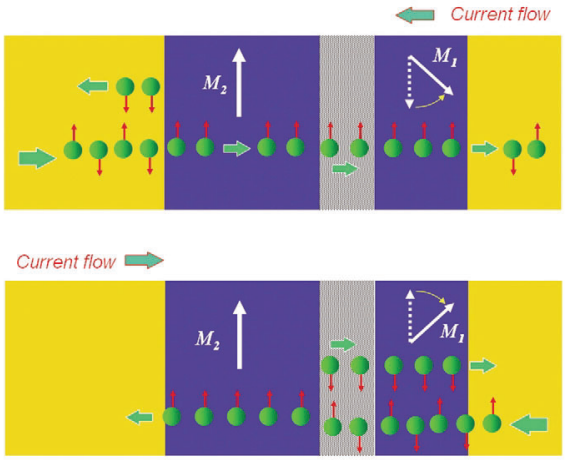

Fig. 17 The spin torque effect, also known as spin momentum transfer. Reversing the current direction reverses the spin polarization direction of the tunneling current. If the electrons flow from layer 2 to layer 1, the effect of spin torque is to rotate the magnetization of layer toward the parallel state. In reversing the direction of tunneling current, the antiparallel state is preferred.

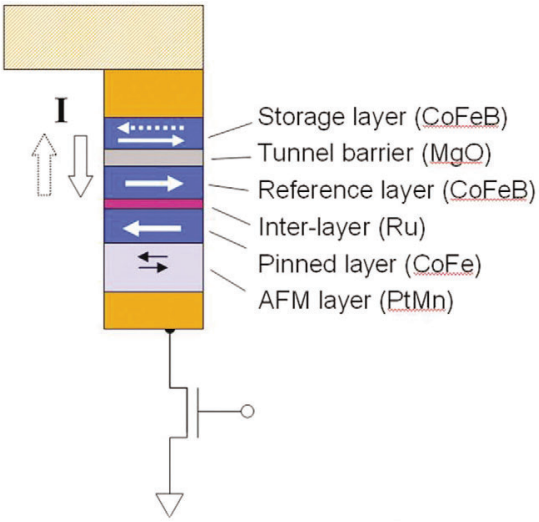

Fig. 18 Schematic of Sony's spin-RAM memory element with direct current injection in which spin torque is used to perform the magnetic switching of the storage layer[56].

sufficient data retention durability. Consequently, the switching threshold, either by magnetic field or spin torque, becomes highly dependent on any geometric, morphological, or physical variations along the edges of the elements, and is one of the key factors that severely limits the scalability of MRAM. MRAM elements with perpendicular magnetization could provide a solution. As shown in Fig. 19, calculations based on spin torque switching, including dynamic micromagnetic modeling, have suggested such a design may enable MRAM to reach many gigabits per chip storage capacity with low operating power[57].

Summary

MTJ research and development has made substantial progress over the past decade, fueled by two current and important commercial applications: HDDs and MRAM. This progress has enabled rapid technological advances in both applications. With the extensive research and development effort we are witnessing, introduction of MgO-based tunnel junctions in commercial products is likely to occur soon. As MTJ technology becomes more mature, we can expect commercialization of many more applications in the near future. mt

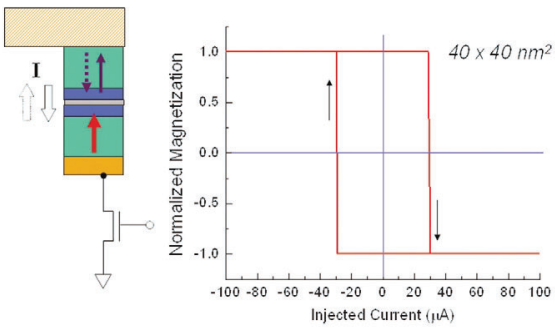

Fig. 19 Calculated magnetic switching of the storage layer of a MTJ memory element by direct current injection using spin torque. The magnetization in the MTJ element is perpendicular and the junction area is 40 nm x 40 nm. The two spin-polarization layers adjacent to the tunnel barrier are assumed to be $Co_{90}Fe_{10}$. A switching current threshold of 30 μA is obtained.

REFERENCES

1. Thomson, W., *Proc. R. Soc. London* (1857) **8**, 546
2. Zhu, J.-G., *Materials Today* (2003) **6** (7-8), 22
3. Baibich, M. N., *et al., Phys. Rev. Lett.* (1988) **61**, 2472
4. Miyazaki, T., *et al., J. Magn. Magn. Mater.* (1991) **98**, L7
5. Plaskett, T. S., *et al., J. Appl. Phys.* (1994) **76**, 6104
6. Moodera, J. S., *et al., Phys. Rev. Lett.* (1995) **74**, 3273
7. Moodera, J. S., *et al., Appl. Phys. Lett.* (1997) **70**, 3050
8. Sousa, R. C., *et al., Appl. Phys. Lett.* (1998) **73**, 3288
9. Cardoso, S., *et al., IEEE Trans. Magn.* (1999) **35**, 2952
10. Moodera, J. S., *et al., Annu. Rev. Mater. Res.* (1999) **29**, 381
11. Yu, J. H., *et al., Appl. Phys. Lett.* (2003) **82**, 4735
12. Wang, D., *et al., IEEE Trans. Magn.* (2004) **40**, 2269
13. Butler, W. H., *et al., Phys. Rev. B* (2001) **63**, 054416
14. Mathon, J., and Umersky, A., *Phys. Rev. B* (2001) **63**, 220403R
15. Bowen, M., *et al., Appl. Phys. Lett.* (2001) **79**, 1655
16. Faure-Vincent, J., *et al., Appl. Phys. Lett.* (2003) **82**, 4507
17. Yuasa, S., *et al., Jpn. J. Appl. Phys.* (2004) **43**, L588
18. Yuasa, S., *et al., Nat. Mater.* (2004) **3**, 868
19. Parkin, S. S. P., *et al., Nat. Mater.* (2004) **3**, 862
20. Yuasa, S., *et al., Appl. Phys. Lett.* (2006) **89**, 042505
21. Djayaprawira, D. D., *et al., Appl. Phys. Lett.* (2005) **86**, 092502
22. Ikeda, S.,*et al., Jpn. J. Appl. Phys.* (2005) **44**, L1442
23. Tsunekawa, K., *et al., IEEE Trans. Magn.* (2006) **42**, 103
24. Simmons, J. G., *J. Appl. Phys.* (1963) **34**, 1793
25. Slonczeski, J. C., *Phys. Rev. B* (1989) **39**, 6995
26. Maekawa, S., and Gäfvert, U., *IEEE Trans. Magn.* (1982) **18**, 707
27. Julliere, M., *Phys. Lett. A* (1975) **54**, 225
28. Soulen, Jr., R. J., *et al., Science* (1998) **282**, 85
29. Monsma, D. J., and Parkin, S. S. P., *Appl. Phys. Lett.* (2000) **77**, 720
30. Ando, Y., *et al., J. Phys. D: Appl. Phys.* (2002) **35**, 2415
31. Sin, K., *et al., IEEE Trans. Magn.* (2000) **36**, 2818
32. Ryan, P., *et al.*, Recording heads for next generation of perpendicular recording. Presented at *The Magnetic Recording Conference 2006*, Pittsburgh, (2006), A1
33. Kobayashi, K., and Akimoto, H., *Fujitsu Sci. Tech. J.* (2006) **42**, 139
34. Park, C., *et al., J. Appl. Phys.* (2006) **99**, 08A901
35. Nishimura, N., *et al., J. Appl. Phys.* (2002) **91**, 5246
36. Park, C., and Zhu, J.-G., unpublished results
37. Zhang, J., and White, R. M., *J. Appl. Phys.* (1998) **83**, 6512
38. Ho, M. K., *et al., IEEE Trans. Magn.* (2001) **37**, 1691
39. Mao, S., *et al., IEEE Trans. Magn.* (2002) **38**, 78
40. Araki, S., *et al., IEEE Trans. Magn.* (2002) **38**, 72
41. Mao, S., *et al., IEEE Trans. Magn.* (2004) **40**, 307
42. Tsunegawa, K., *et al.*, CoFeB/MgO/CoFeB magnetic tunnel junctions with high TMR ratio and low junction resistance. Presented at *Int. Magn. Conf.*, Nagoya, Japan, (2005), FB-05
43. Mao, S., *et al., IEEE Trans. Magn.* (2006) **42**, 97
44. Kagami, T., *et al., IEEE Trans. Magn.* (2006) **42**, 93
45. Engel, B. N., *et al., IEEE Trans. Nano.* (2002) **1**, 32
46. Tehrani, S., *et al., Proc. IEEE* (2003) **91**, 703
47. Engel, B. N., *et al., IEEE Trans. Magn.* (2005) **41**, 132
48. De Voss, M., Analysis: Freescale's MRAM ready to fly?, *EE Times* (July 20, 2006)
49. Dave, R. W., *et al., IEEE Trans. Magn.* (2006) **42**, 1935
50. Slonczewski, J. C., *J. Magn. Magn. Mater.* (1996) **159**, L1
51. Berger, L., *Phys. Rev. B* (1996) **54**, 9353
52. Myers, E. B., *et al., Science* (1999) **285**, 867
53. Koch, R. H., *et al., Phys. Rev. Lett.* (2004) **92**, 088302
54. Braganca, P. M., *et al., Appl. Phys. Lett.* (2005) **87**, 112507
55. Huai, Y., *et al., IEEE Trans. Magn.* (2005) **41**, 2621
56. Hosomi, M., *et al., Tech. Dig. IEDM* (2005), 459
57. Zhu, X., and Zhu, J.-G., *IEEE Trans. Magn.* (2006), in press